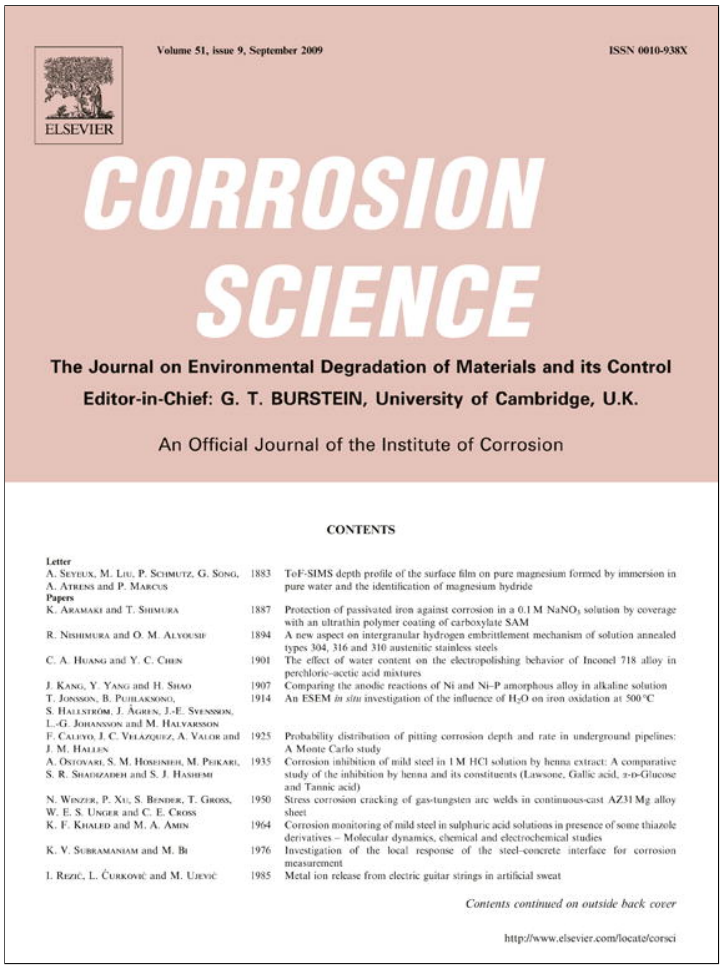

Volume 51, issue 9, September 2009 ISSN 0010-938X

ELSEVIER

CORROSION SCIENCE

The Journal on Environmental Degradation of Materials and its Control

Editor-in-Chief: G. T. BURSTEIN, University of Cambridge, U.K.

An Official Journal of the Institute of Corrosion

CONTENTS

Contents continued on outside back cover

http://www.elsevier.com/locate/corsci

Corrosion Science 51 (2009) 2158–2164

Contents lists available at ScienceDirect

Corrosion Science

journal homepage: www.elsevier.com/locate/corsci

Corrosion behavior of nitrogen doped diamond-like carbon thin films in NaCl solutions

N.W. Khun [a], E. Liu [a,*], X.T. Zeng [b]

[a] School of Mechanical and Aerospace Engineering, Nanyang Technological University, 50 Nanyang Avenue, Singapore 639798, Singapore
[b] Singapore Institute of Manufacturing Technology, 71 Nanyang Drive, Singapore 638075, Singapore

ARTICLE INFO

Article history:
Received 25 March 2009
Accepted 29 May 2009
Available online 9 June 2009

Keywords:
A. Sputtered film
B. Polarization
C. Corrosion

ABSTRACT

Nitrogen doped tetrahedral amorphous carbon (ta-C:N) thin films were grown on p-Si(1 1 1) substrates using filtered cathodic vacuum arc (FCVA) deposition by varying nitrogen flow rate. The effect of nitrogen flow rate on the corrosion performance of the films was investigated through potentiodynamic polarization and immersion tests in 0.6 M NaCl solutions. The polarization results showed that the corrosion resistance of the films dropped with increased nitrogen flow rate due to formation of more sp^2 bonds. The immersion tests revealed that the pH value of the solutions had a significant effect on the corrosion behavior of the ta-C:N films.

1. Introduction

Diamond-like carbon (DLC) forms suitable candidate materials for use in harsh environments. A unique combination of high hardness, low friction and wear, and high chemical inertness of DLC materials makes them ideal protective coatings in corrosive environments. The characteristics of DLC films can be altered by incorporating different elements such as H, N, F, Si and some metals (e.g. Ti, V) in the films [1–3]. For example, by introducing nitrogen into DLC (DLC:N) films, the films can become an n-type semiconductor with a significant electrical conductivity [4]. Rodil et al. reported that nitrogen atoms in CN_x films could be preferentially π bonded in both aromatic and non-aromatic structures [5]. The decreases of sp^3 content, density and stress of DLC:N films with respect to increased nitrogen pressure applied during film deposition were observed by Polo et al. [6].

Although DLC films are usually electrochemically nobler than substrates, the presence of nanopores in the films can lead to the electrochemical dissolution of the substrates due to permeation of water, environmental oxygen and ions. Corrosion usually initiates at imperfections, pinholes, places of large compositional inhomogenity or sites with induced stresses. The properties that directly influence the corrosion behavior of DLC films are film structure, uniformity, adhesion to substrate, surface roughness, and electrical conductivity.

DLC films can offer a good protection of metallic substrates from corrosion [7–10]. Introduction of Si into DLC films can lead to a significant improvement of the corrosion resistance of the films by increasing charge transfer resistance and decreasing anodic current in polarization, which could be attributed to the formation of a denser coating, thus impeding the penetration of water molecules or ions [11,12].

The porosity density is one of the most important parameters in assessing the effectiveness of corrosion protection of DLC films. It was reported that nanoporosity density increased with prolonged immersion time [13]. Moreover, Papakonstantinou et al. [14] found that the corrosion resistance of ultra-thin DLC films substantially increased with immersion time in an electrolytic solution due to the filling of pores with a passivating material that prevents the access of the electrolyte to the substrate. Sharma et al. [15] also found that the corrosion resistance of DLC films was increased by increasing the thickness of the films.

Liu et al. [16] reported that the adhesion strength of DLC films influenced the corrosion protection of the films, i.e., the higher the adhesion strength of a film, the better the corrosion resistance of the film was. A sufficient adhesion of a DLC film to its substrate can reduce the undermining effect from corrosive media, thus enhancing the corrosion resistance of the film.

Moreover, deposition techniques such as magnetron sputtering and filtered cathodic vacuum arc (FCVA) can affect the corrosion resistance of DLC films. Compared to sputtering method, FCVA method can produce higher fractions of sp^3 bonds in DLC films, which is expected to be able to prevent prompt dissolution of the films in corrosive media.

Nitrogen doped tetrahedral amorphous carbon (ta-C:N) is a type of DLC with higher density and sp^3 content. This paper is focused on the effect of nitrogen flow rate used during film deposition on the corrosion behavior of ta-C:N films.

* Corresponding author. Tel.: +65 6790 5504; fax: +65 6792 4062.
E-mail address: MEJLiu@ntu.edu.sg (E. Liu).

0010-938X/$ - see front matter © 2009 Elsevier Ltd. All rights reserved.
doi:10.1016/j.corsci.2009.05.050

2. Experimental details

Nitrogen doped tetrahedral amorphous carbon (ta-C:N) films were deposited on boron-doped p-type (1 1 1) silicon wafers (1–6×10^{-3} Ω cm) using a filtered cathodic vacuum arc (FCVA) deposition system (Nanofilms) at room temperature. A pure graphite target (⩾99.95% C) was used as the C source, and nitrogen gas was introduced by a mass flow controller into the deposition chamber at varying nitrogen flow rate from 0.5 to 20 sccm. A substrate bias (pulse) of 1500 V was applied during all the film depositions.

The structure of the films was measured with a Confocal Micro Raman Spectroscope (Renishaw 1000) using 632 nm line excited by a He–Ne laser over the range of 800–2000 cm^{-1}. An objective lense (×50) was used for a better signal-to-noise ratio. The Raman instrument used had a spectral resolution of 1 cm^{-1} and a spatial resolution of 1 μm.

The surface morphology of the samples was measured with atomic force microscopy (AFM) (Digital Instruments, S-3000) using a tapping mode Si_3N_4 cantilever with a scan size of 1×1 μm^2 and scanning electron microscopy (SEM) (JEOL-JSM-5600LV). For surface roughness (Ra) measurement with AFM, five measurements were randomly conducted on each sample and an average value was taken.

The adhesion strength of the films was studied with a micro-scratch tester (Shimadzu SST-101) having a diamond stylus of 15 μm in diameter under a progressive loading condition at room temperature. The scan amplitude, frequency, scratch rate, and down speed for all the tests were set as 50 μm, 30 Hz, 10 μm/s, and 2 μm/s, respectively. Five measurements were conducted on each sample and an average value of critical load was taken.

Potentiodynamic polarization measurements of the ta-C:N films were carried out using a potentiostat/galvanostat station (EG & G 263A) with a standard three-electrode electrochemical cell (K0235, Princeton Applied Research) containing a 0.6 M NaCl solution at a fixed scan rate of 0.8 mV/s (352SoftCorr III) at room temperature. The polarization data were then fitted using a nonlinear least-squares fitting (PARCalc) to determine corrosion potentials (E_{corr}) and currents (I_{corr}). For the polarization testing, the ta-C:N film coated specimens were cut into 2×2 cm^2 square pieces and a gold layer was deposited onto the backsides of the cut samples to make them in good electrical connection during the polarization measurements. The tested area on the films was a circle of 1 cm in diameter. The polarization potentials were measured with respect to a saturated standard calomel reference electrode (SCE) in a saturated KCl solution (244 mV vs. SHE at 25 °C). A platinum mesh was used as the counter electrode.

Immersion tests of the ta-C:N film coated samples were performed in 0.6 M NaCl solutions with different pH values compensated by HCl ($HCl \rightarrow H^+ + Cl^-$) and NaOH ($NaOH \rightarrow Na^+ + OH^-$) for 366 h at room temperature. For the immersion tests, the specimens were cut into 1×1 cm^2 square pieces that were then directly immersed and suspended in the corrosive media without any packaging.

3. Results and discussion

The FCVA process can generate high kinetic energy of impinging carbon species that in turn form ta-C films with a high fraction of sp^3 bonds. As shown in Fig. 1, the Raman spectra of the films correspond to the sp^2 bonded carbon embedded in the sp^3 networks. It is well known that a typical Raman spectrum of DLC is composed of G and D bands, in which the G band is due to the stretching vibrations of any pairs of sp^2 sites in chains or aromatic rings and the D band comes from the breathing mode of those sp^2 sites

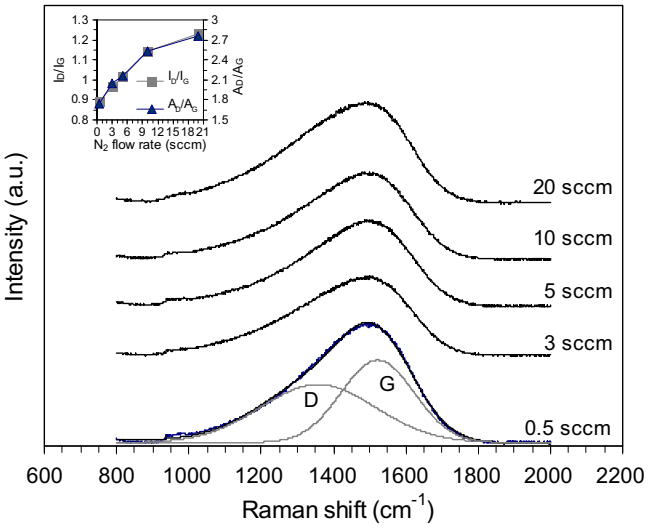

Fig. 1. Raman spectra of ta-C:N films deposited with different nitrogen flow rates. The inset shows I_D/I_G and A_D/A_G as a function of nitrogen flow rate.

only in aromatic rings [17]. Ferrari et al. proposed [17] that sp^2 bonds could exist not only as rings but also as chains in a dense matrix of DLC depending on its sp^3 content. Usually, the introduction of nitrogen into a carbon network induces the formation of new sp^2 sites and encourages the sp^2 sites to form clusters because of preferential π bonding of nitrogen [5]. Therefore, the increased nitrogen content in the ta-C:N films enhances the amount and clustering of the sp^2 sites. The increased intensity ratio (I_D/I_G) and integrated area ratio (A_D/A_G) between D and G peaks fitted using a Gaussian function for the G peaks and a Lorentzian function for the D peaks with increased nitrogen flow rate (inset in Fig. 1) reveal that the increase of nitrogen content in the ta-C:N films promotes the clustering of the aromatic rings indicating an increase in graphitic phases [18,19].

In a scratch test, a critical load is determined when an abrupt change in tangential force is observed, which comes from an instant failure between DLC film and Si substrate. The critical loads for the ta-C:N film coated samples increase from 445 to 477 mN with increased nitrogen flow rate as shown in Fig. 2a. It is well known that the adhesive strength of a film is also strongly influenced by its residual stress. Sullivan and co-workers [20] proposed that the reduction in residual stress was due to the conversion of a small fraction of sp^3 sites to sp^2 sites during the film deposition. The sp^2 bonds having shorter bond lengths than those of the sp^3 bonds would reduce the strains in the film plane. In addition, since the C═N bonds have shorter bond lengths compared to the C—C and C═C bonds, the increase of the C═N bonds with higher nitrogen flow rates also gives rise to a higher critical load by reducing the strain in the film [21].

The inset in Fig. 2b shows the load-cartridge output signal from the scratch test of the specimen with the ta-C:N film deposited with 0.5 sccm N_2, from which a critical load of 456 mN is determined. A cartridge output signal is a voltage ratio obtained from the motions of the stylus and the cartridge that is also oscillating horizontally above the sample during the scratch testing [22]. The cartridge output signals are an indication of tangential forces experienced by the stylus during the scratch testing. No fluctuation can be seen on the cartridge output signals with respect to normal load, except for an abrupt increase of the critical load. A stable linear relationship between tangential force and normal load indicates a uniform film adhesion throughout the film-substrate interface. From the SEM micrograph (Fig. 2b), no cohesive failure

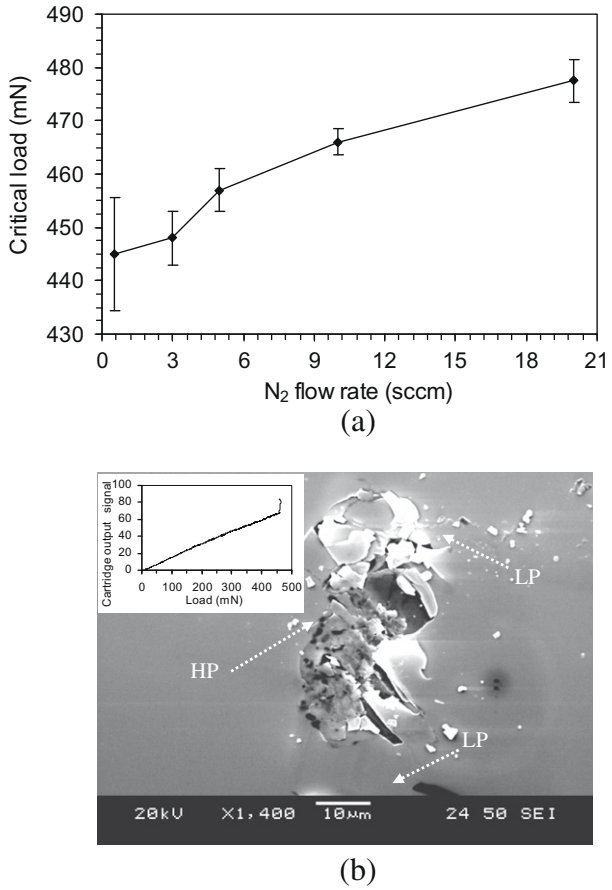

Fig. 2. (a) Critical loads of ta-C:N films with respect to nitrogen flow rate and (b) SEM micrograph of a ta-C:N film (0.5 sccm N_2) scratch-tested till a critical load of 456 mN. HP and LP indicate high pressure and low pressure areas, respectively. The inset is the progressive loading curve measured, from which the critical load is determined.

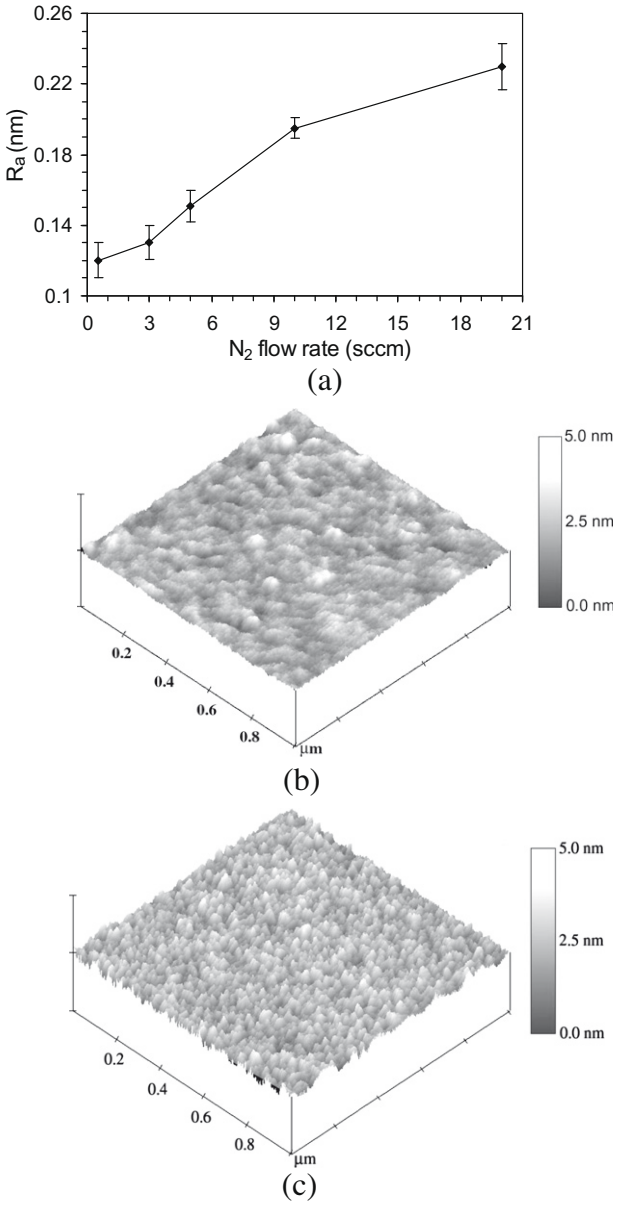

Fig. 3. Ra values of ta-C:N films vs. nitrogen flow rate (a) and AFM images of ta-C:N films deposited with two different nitrogen flow rates: (b) 0.5 and (c) 20 sccm.

of the film can be found within the scratched path of the film, while only the fractured area with flaking at the critical load can be viewed as a brittle fracture. It implies that a high fraction of sp^3 bonds can enhance the cohesive strength of the ta-C:N films so that the fracture occurs only at the critical load. This is in agreement with the work by Gupta et al., in which a thinner film exhibited an instant damage when the normal load exceeded the critical load [23]. When the cartridge vibrates, the stylus is pulled in the direction of the vibration. The traction induced results in a non-uniform pressure distribution that causes the shearing between the film and substrate, leading to the peeling-off and breaking of the film. The adhesion strength of the film to the substrate also contributes to the fractured film surface morphology. A non-uniform pressure distribution explains why the fractured area is larger than the diameter of the diamond indenter tip as seen in Fig. 2.

When the nitrogen flow rate changes from 0.5 to 20 sccm, the surface roughness (Ra) of the ta-C:N films slightly increases from about 0.12 nm to about 0.23 nm as shown in Fig. 3(a). It indicates that increasing nitrogen flow rate increases the surface roughness of the ta-C:N films due to a reduced density of the films caused by increased sp^2 sites [21]. In addition, the aggregation of the nitrogen inclusions in the ta-C:N films also contributes to the surface roughness of the films due to the difference in electronegativity values between carbon (~2.55, pauling scale) and nitrogen (~3.04) [21]. The ta-C:N film deposited with 0.5 sccm N_2 has fine asperities as shown in Fig. 3(b), which is due to a higher fraction of sp^3 carbon bonding formed in the film. Larger surface asperities can be seen on the ta-C:N film deposited with 20 sccm N_2 (Fig. 3(c)), which are possibly caused by the increased number of sp^2 sites and aggregation of nitrogen atoms [24,25].

Fig. 4 presents the potentiodynamic polarization curves for the ta-C:N films as a function of nitrogen flow rate. From the curves, it is found that the cathodic branches do not change with nitrogen flow rate except for the sample deposited with 3 sccm N_2. However, the bonding structure of ta-C:N films, which varies with nitrogen flow rate, affects the anodic branches of their polarization curves. It shows that the ta-C:N film deposited with 3 sccm N_2 has the highest corrosion resistance.

In the polarization curves of the ta-C:N films deposited with 0.5 and 3 sccm N_2, a reduction in corrosion current is found at a potential above 500 mV vs. SCE. However, no such a reduction in corrosion current is found from the rest curves, which can be explained based on the observation of the surface morphologies of the corroded films. Fig. 5(a) and (b) shows the SEM micrographs of the corroded areas of the ta-C:N films deposited with 0.5 and 3 sccm N_2, respectively, after the polarization testing in the 0.6 M NaCl

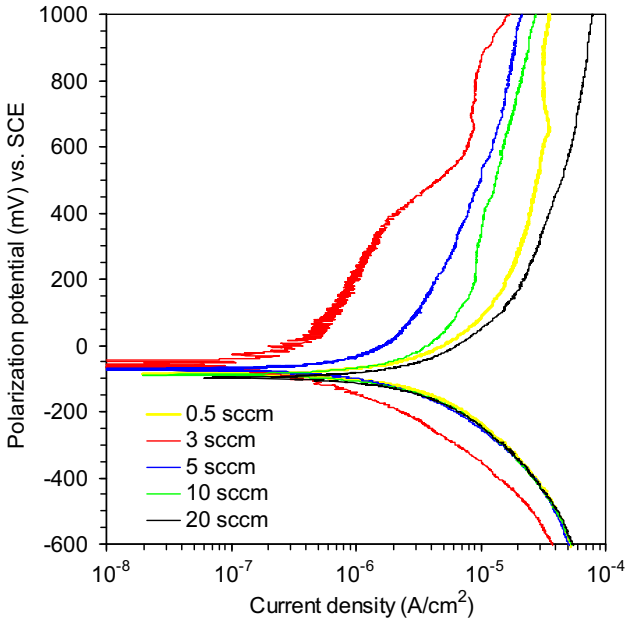

Fig. 4. Potentiodynamic polarization curves of ta-C:N films measured in a 0.6 M NaCl solution at room temperature.

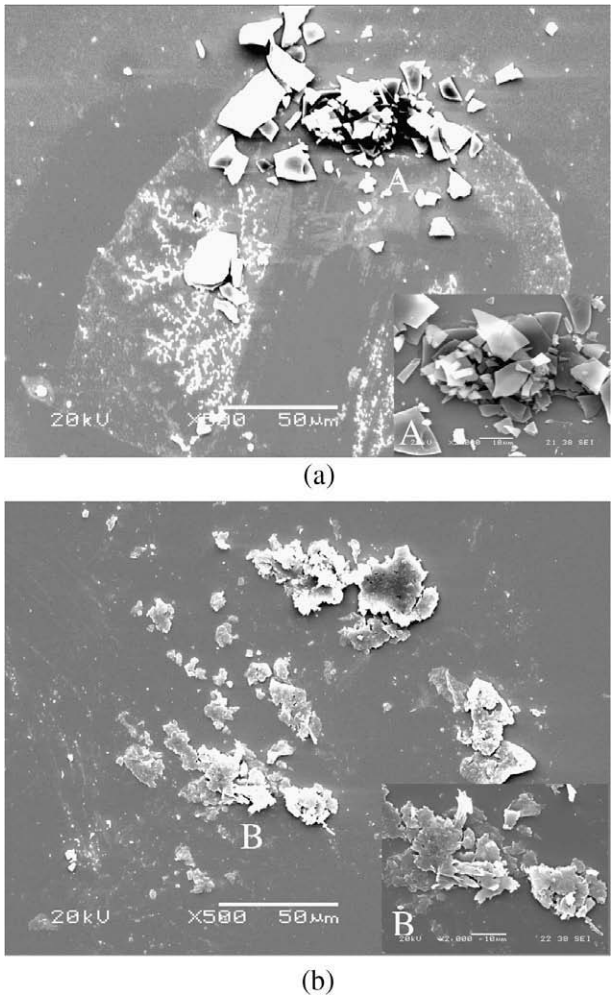

Fig. 5. SEM micrographs showing surface morphologies of ta-C:N films after potentiodynamic polarization tests: (a) 0.5 sccm, E_{corr} = -85.72 mV vs. SCE and (b) 3 sccm, E_{corr} = −57.41 mV vs. SCE, where the insets in the bottom right corners show the respective enlarged views of locations A and B.

solution at room temperature. Some localized solid products can be seen on the film surfaces, which usually agglomerate around the defects or pores. These solid products would reduce the corrosion current by blocking the diffusion paths of the electrochemically active species from the electrolytic solution to the film surface or to the underlying substrate. That the reduction of the corrosion current after the formation of these solid products takes place is consistent with the decreased anodic currents in the anodic branches of the polarization curves of the ta-C:N films deposited with 0.5 and 3 sccm N_2 (insets of Fig. 5).

In Fig. 6, the corrosion potentials (E_{corr}) of the ta-C:N films are determined by fitting the potentiodynamic polarization curves measured at the fixed scan rate of 0.8 mV/s (Fig. 4). The corrosion current (I_{corr}) and anodic (β_a) and cathodic (β_c) Tafel slopes are determined at the same time. The polarization resistance (R_p) values in Fig. 6 are then calculated using the following formula [26]:

$$R_p = \beta_a\beta_c/2.3I_{corr}(\beta_a + \beta_c) \quad (1)$$

where R_p is in kΩ cm^2; β_a and β_c are in terms of V/I-decade; and I_{corr} is in μA/m^2.

It is found that the trend of R_p is similar to that of E_{corr} as shown in Fig. 6. When the nitrogen flow rate is increased from 0.5 to 3 sccm, the E_{corr} shifts from −85.7 to −57.4 mV vs. SCE and the R_p increases from 16.8 to 150.1 kΩ cm^2. However, the E_{corr} shifts to more negative values from −57.4 to −97.6 mV vs. SCE and the R_p turns to decrease from 150.1 to 15.8 kΩ cm^2 with further increased nitrogen flow rate to 20 sccm. The corrosion results point out that the ta-C:N film deposited with 3 sccm N_2 shows the highest corrosion resistance among the films used in this study.

The decreased corrosion resistance of the ta-C:N films with higher nitrogen flow rates than 3 sccm is attributed to several factors such as the bonding structure, electrical resistivity, surface roughness and porosity density of the films. An increase of nitrogen content in the films promotes the graphitic phases as depicted by the increased I_D/I_G and A_D/A_G ratios (inset of Fig. 1). The increased graphitic phases in the amorphous carbon structure lead to an earlier dissolution of the films.

In addition, the corrosion properties of the ta-C:N films are related to the kinetics of electrochemical reactions taking place at the film-solution interface. It is known that the introduction of nitrogen into the films reduces the electrical resistivity of the films [4,18,27,28]. Another parameter which can determine the electrical conductivity of the ta-C films is sp^2/sp^3 ratio, i.e. the higher the sp^2/sp^3 ratio, the lower the electrical resistivity of the film is [29]. The increased electrical conductivity of the ta-C:N films with increased nitrogen flow rate promotes the electron transfer to or from the films during the corrosion testing, thus accelerating the electrochemical reactions in the electrical double layers (EDL).

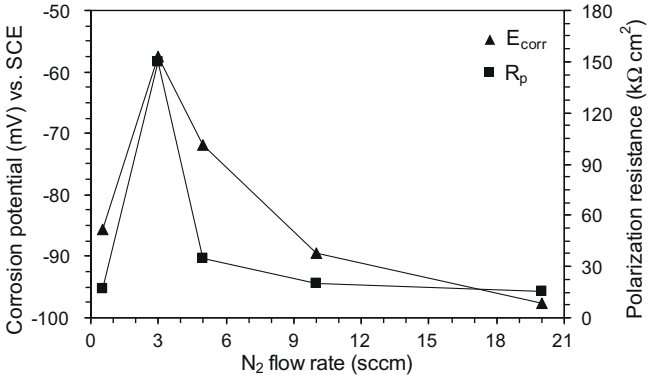

Fig. 6. Corrosion potentials (E_{corr}) and polarization resistances (R_p) of ta-C:N films as a function of nitrogen flow rate.

Moreover, due to the presence of many tiny anodic and cathodic sites on the surface of the films caused by the aggregated nitrogen or the electrochemical potential difference between the films and substrates [16,24,30], a galvanically induced corrosion could occur between them after the electrochemically active species access the film surface and permeate into the substrate through the pores. Such corrosion becomes pronounced with higher nitrogen flow rates.

Furthermore, the increased surface roughness of the ta-C:N films also contributes to the decreased corrosion resistance of the films because of a larger exposed surface area to the electrolyte during the corrosion testing.

These combined effects have resulted in the corrosion behavior of the ta-C:N films as shown in Fig. 6. A lower corrosion resistance of the ta-C:N film deposited with 0.5 sccm N_2 than that of the film deposited with 3 sccm N_2 may be attributed to more porosities formed in the film deposited with 0.5 sccm N_2, which probably results from an unbalance between the kinetic energy of the sputtered C species arriving at the film growing surface and the surface mobility of the adatoms on the growing surface [31,32]. An increase of nitrogen gas in the deposition chamber under the fixed argon flow rate reduces the mean free path of the sputtered species, thus decelerating the kinetics of the sputtered species and lessening the formation of porosities. Above combined factors can explain the higher corrosion resistance of the ta-C:N film deposited with 3 sccm N_2 than that of the one deposited with 0.5 sccm N_2.

Immersion test offers a simple and cheap way of studying the corrosion behavior of the ta-C:N films immersed in the corrosive media for a longer time. In this investigation, the ta-C:N film coated samples (3 sccm N_2) were immersed in the 0.6 M NaCl solutions with different pH values compensated with HCl ($HCl \rightarrow H^+ + Cl^-$) and NaOH ($NaOH \rightarrow Na^+ + OH^-$) for 336 h. Fig. 7 shows the surface morphologies of the samples after the immersion tests where no detachment of the film is found. The sample immersed in a solution of pH 2 is more severely corroded than other two samples tested in the solutions of pH 4.5 and pH 12, because of unbalanced hydrogen and hydroxide ions in the solutions [30]. The corrosion on the surface comes from the reaction of the film with the electrochemically active species in the electrolyte. When the ta-C:N film atoms (e.g. $C \rightarrow C^{2+} + 2e^-$) are dissolved as ions into the aqueous solution, the electrons released will flow to the electrochemically active species in the solution where the hydrogen ions resulting from the water dissociation ($H_2O \rightarrow OH^- + H^+$) gain these released electrons to form hydrogen gas in the cathodic reaction ($H^+ + e^- \rightarrow H$, $2H \rightarrow H_2$) [33]. At $pH < 7$, the H^+ ions mainly influence the corrosion while at $pH \geqslant 7$, the OH^- ions deplete the H^+ ions in the solution through hydrolysis resulting in a reduced corrosion. Therefore, an apparent change in corrosion characteristics on the surface of the ta-C:N film

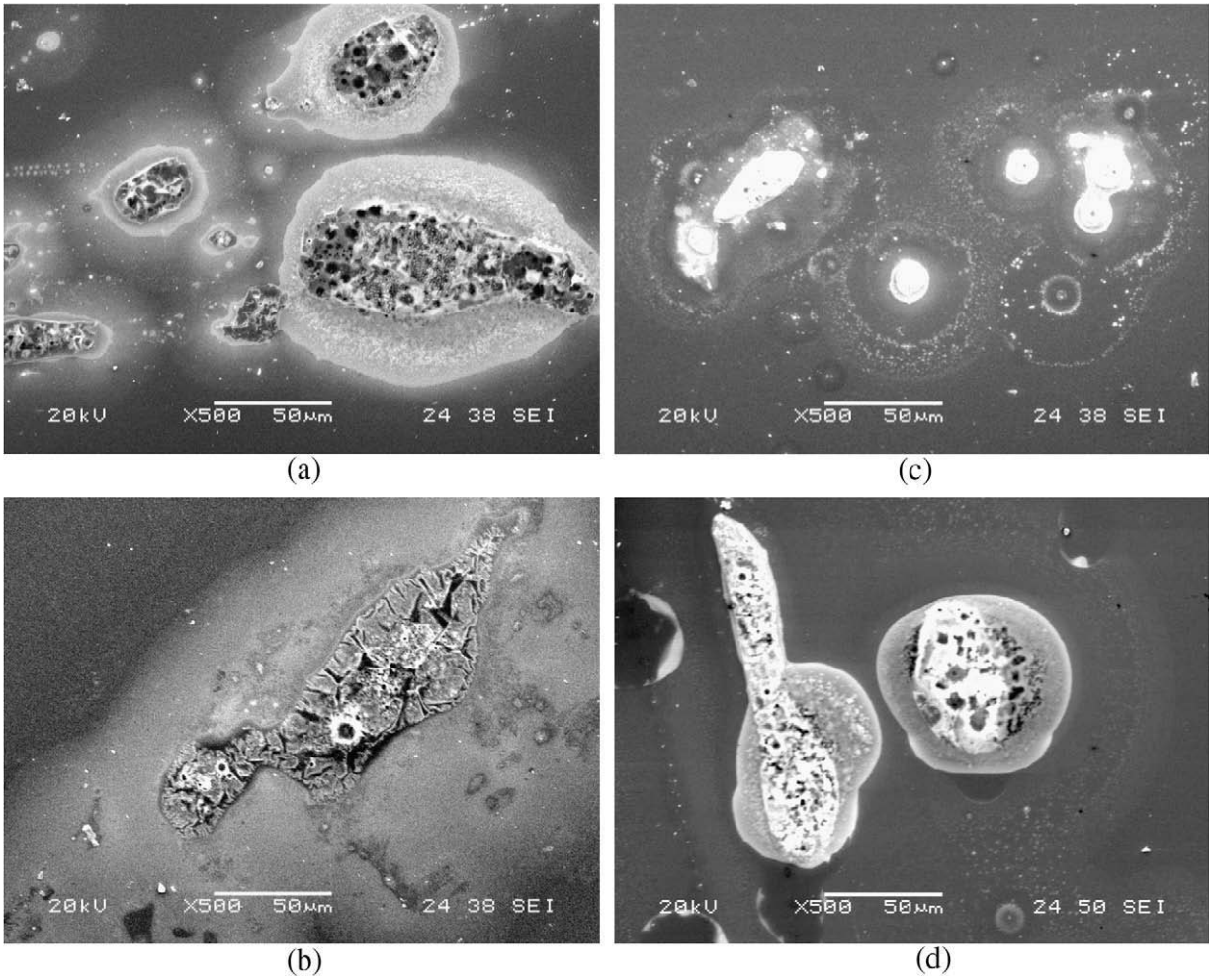

Fig. 7. SEM micrographs of the corroded areas of ta-C:N film coated samples after immersion tests in 0.6 M NaCl solutions with different pH values: (a) pH 2, (b) pH 4.5 and (c) pH 12 for the film deposited with 3 sccm N_2 and (d) pH 4.5 for the film deposited with 20 sccm N_2 for comparison. All the tests are conducted for 336 h at room temperature and ambient atmosphere.

with respect to pH value is observed in the SEM micrographs (Fig. 7a–c).

At the same time, the effect of Cl^- ions, which are increased by compensating the solution with HCl to make the solution more acidic, on the corrosion resistance of the ta-C:N films should also be taken into account besides the effect of H^+ ions. Since the catalytic activity of the Cl^- ions accelerates the corrosion process of the ta-C:N films, it should be noted that the increase in the concentration of the Cl^- ions with the compensation of the solution can give an additional effect on the decrease in the corrosion resistance of the films with decreased pH as discussed above.

The initiation of a pit on the film surface occurs when a small local site on the film is exposed to the damaging species such as chloride and hydrogen ions. It is known that the pits initiate at defects, surface compositional heterogeneities and porosities because these imperfections degrade the cross-linking structure of the film. The ta-C films may always contain certain open pores that allow a direct access of the electrolyte to the underlying substrate and some closed pores which are not absolutely open or which diameters are only big enough to allow some specific ions or molecules in the electrolyte to gradually migrate to the substrate surface [13]. When the electrolyte accesses the film surface, the pores become the initiation sites for the corrosion. An increase in immersion time causes the closed pores to become open and the open pores to grow, resulting in an increase of the porosity density in the film. The pores serving as crevices allow the entrapment of the permeated electrochemically active species inside them and a buildup of the positive hydrogen ions through hydrolytic reactions. The buildup of the positive hydrogen ions increases the acidity of the entrapped electrolyte inside the pores when the openings of the pores are covered with the corrosion products resulted from the corrosion of the film. In addition, such a buildup of the positive charges in the pores becomes a strong attractor to negative ions, e.g. chlorine, which can be corrosive in their own right, resulting in a more severe corrosion inside the pores than the surrounding. Eventually, the growth of the pores by connecting adjacent pores forms the pits as shown in Fig. 7a. However, a collection of the pits (Fig. 7a), which serves as an active site with respect to the surrounding (a cathodic site) and shows a more severe corrosion than the surrounding, indicates that the localized occurrence of the pits probably results from the aggregation of nitrogen in the amorphous carbon structure. The aggregated nitrogen locally degrades the sp^3 bonded cross-link structure through the increased sp^2 sites and the degraded cross-link structure can be easily attacked by the electrochemically active species. As explained above, the insufficient repassivation of the film also accelerates the localized dissolution of the film. When the pH value of the electrolyte is decreased, the increased concentration of hydrogen ions increases the acidity of the electrolyte accessible to the ta-C:N film as well as the entrapped electrolyte inside the pores, thus accelerating the growth of the pits. Therefore, after the immersion tests, a more apparent pitting of the ta-C:N sample (3 sccm N_2) is found with the solution of pH 2 (Fig. 7a) than those tested with the solutions of pH 4.5 (Fig. 7b) and pH 12 (Fig. 7c).

A ta-C film is usually electrochemically nobler than a Si substrate, so a galvanically induced corrosion can occur between the film and the substrate when the electrolyte has permeated into the substrate through some pores or defects of the film [13]. The increased electrical conductivity of the film with nitrogen doping may facilitate the galvanically induced corrosion between the film and the substrate. With a prolonged immersion, more oxygen existing in the electrolyte confined within the pores and undermining areas of the film is consumed leading to an increase in concentration of H^+ ions in the entrapped electrolyte. The accumulated H^+ ions can attract the negatively charged ions like chlorine ions in the surrounding electrolyte. A highly acidic local environment with increased immersion time can cause a substantial increase in corrosion rate, resulting in large undermining areas. The increased electrolyte trapped inside the enlarged undermining areas leads to a higher surface tension and eventually cracking and damaging happen to the film as revealed in Fig. 7(b) for the ta-C:N film (3 sccm N_2). From the comparison between Fig. 7b and d, the ta-C:N film deposited with a higher N_2 flow rate (20 sccm) has a lower undermining effect due to its higher adhesion strength and at the same time, however, a higher pitting rate attributed to a higher nitrogen doping level. Therefore, it can be deduced that the adhesive strength of the films is an important parameter to lessen the undermining effect of the imperfections in the films exposed to the corrosive media.

4. Conclusions

The effects of nitrogen incorporation in the ta-C:N films on the microstructure, adhesive strength, surface roughness and corrosion behavior of the films were investigated. The surface roughness of the films increased with nitrogen flow rate due to the aggregation of nitrogen atoms in the films. As found from the potentiodynamic polarization experiments, the corrosion resistance of the ta-C:N films decreased with increased nitrogen flow rate because of the increased sp^2 fractions in the ta-C:N films. The increase of N content in the ta-C:N films increased the electrical conductivity of the films, which in turn accelerated the electron transfer kinetics affecting the corrosion rate of the films. The immersion tests were employed to study the corrosion behavior of the ta-C:N films in similar media for long runs. It was observed that the pH value of the solutions affected the anti-corrosion performance of the ta-C:N films, i.e., the lower the pH value, the more severe the corrosion of the film was.

Acknowledgements

This work was supported by the research grant (EWI-0601-IRIS-035-00) from the Environment & Water Industry Development Council (EWI), Singapore. N.W. Khun is grateful for the Ph.D. scholarship from the Nanyang Technological University (NTU), Singapore.

References

[1] C. Du, X.W. Su, F.Z. Cui, X.D. Zhu, Biomaterials 19 (1998) 651.
[2] G. Francz, A. Schroeder, R. Hauert, Surf. Interf. Anal. 28 (1999) 3.
[3] R. Hauert, U. Mueller, G. Francz, F. Birchler, A. Schroeder, J. Mayer, E. Wintermantel, Thin Solid Films 308–309 (1997) 191.
[4] A. Zeng, E. Liu, S.N. Tan, S. Zhang, J. Gao, Electroanalysis 14 (2002) 1110.
[5] S.E. Rodil, S. Muhl, Diam. Relat. Mater. 13 (2004) 1521.
[6] M.C. Polo, J.L. Andujar, A. Hart, J. Robertson, W.I. Milne, Diam. Relat. Mater. 9 (2000) 663.
[7] B. Tomcik, S.C. Seng, B. Balakrisnam, J.Y. Lee, Diam. Relat. Mater. 11 (2002) 1409.
[8] M.A.S. Oliveira, A.K. Vieira, M. Massi, Diam. Relat. Mater. 12 (2003) 2136.
[9] E.T. Uzumaki, C.S. Lambert, W.D. Belangero, C.M.A. Freire, C.A.C. Zavaglia, Diam. Relat. Mater. 15 (2006) 982.
[10] G.F. Huang, L.P. Zhou, W.Q. Huang, L.H. Zhao, S. Li, D.Y. Li, Diam. Relat. Mater. 12 (2003) 1406.
[11] P. Papakonstantinou, J.F. Zhao, P. Lemoine, E.T. McAdams, J.A. McLaughlin, Diam. Relat. Mater. 11 (2002) 1074.
[12] H.G. Kim, S.H. Ahn, J.G. Kim, S.J. Park, K.R. Lee, Diam. Relat. Mater. 14 (2005) 53.
[13] A. Zeng, E. Liu, I.F. Annergren, S.N. Tan, S. Zhang, P. Hing, J. Gao, Diam. Relat. Mater. 11 (2002) 160.
[14] P. Papakonstantinou, J.F. Zhao, A. Richardot, E.T. McAdams, J.A. McLaughlin, Diam. Relat. Mater. 11 (2002) 1124.
[15] R. Sharma, P.K. Barhai, N. Kumari, Thin Solid Films 516 (2008) 5397.
[16] C.L. Liu, D.P. Hu, J. Xu, D.Z. Yang, M. Qi, Thin Solid Films 496 (2006) 457.
[17] A.C. Ferrari, J. Robertson, Phys. Rev. B 20 (61) (2000) 14095.
[18] J. Robertson, Mate. Sci. Eng. 37 (2002) 129.
[19] S.S. Roy, P. Papakonstantinou, R. McCann, G. Abbas, J.P. Quinn, J.A. McLaughlin, Diam, Relat. Mater. 13 (2004) 1459.
[20] J.P. Sullivan, T.A. Friedmann, A.G. Baca, J. Electron. Mater. 26 (1997) 1021.
[21] N.W. Khun, E. Liu, H.W. Guo, Electroanalysis 17 (2008) 1851.

[22] N. Akita, Y. Konishi, S. Ogura, M. Imamura, Y.H. Hu, X. Shi, Diam. Relat. Mater. 10 (2001) 1017.
[23] B.K. Gupta, B. Bhushan, Thin Solid Films 170 (1995) 391.
[24] E. Liu, X. Shi, H.S. Tan, L.K. Cheah, Z. Sun, B.K. Tay, J.R. Shi, Surf. Coat. Tech. 120–121 (1999) 601.
[25] H. Ma, L. Zhang, N. Yao, B. Zhang, H. Hu, G. Wen, Diam. Relat. Mater. 9 (2000) 1608.
[26] B. Bhushan, Tribology and Mechanics of Magnetic Storage Devices, 2nd ed., Springer, New York, 1996.
[27] L.X. Liu, E. Liu, Surf. Coat. Tech. 198 (2005) 189.
[28] N.W. Khun, E. Liu, Electrochim. Acta 54 (2009) 2890.
[29] W. Cai, J.H. Sui, Surf. Coat. Tech. 201 (2007) 5194.
[30] B. Tomcik, T. Osipowicz, J.Y. Lee, Thin Solid Films 360 (2000) 173.
[31] S. Mahieu, P. Ghekiere, D. Depla, R. De Gryse, Thin Solid Films 515 (2006) 1229.
[32] J. Seth, R. Padiyath, S.V. Babu, Diam. Relat. Mater. 3 (1994) 210.
[33] B. Tomcik, S.C. Seng, B. Balakrisnan, J.Y. Lee, Diam. Relat. Mater. 11 (2002) 1409.